Supplement of Biogeosciences, 22, 3821–3842, 2025
https://doi.org/10.5194/bg-22-3821-2025-supplement

Biogeosciences
Open Access

Supplement of

Lake anoxia, primary production, and algal community shifts in response to rapid climate changes during the Late Glacial

Stan J. Schouten et al.

Correspondence to: Stan J. Schouten (stan.schouten@unibe.ch)

S1: HPLC analysis and chromatogram evaluation

Settings for HPLC analysis

We deployed two mobile phases; Mobile-phase A: volumetric ratio of 2:8, milliQ:methanol with ion-pairing (0.001 M tetrabutyl ammonium phosphate and 0.001 M propionic acid) and Mobile phase B: volumetric ratio of 6:4, acetone:methanol. The HPLC protocol follows Lami et al. (2000). We injected 100 µl of pigment extract into a mobile phase A and ramped in the first 30 min from 85% mobile-phase A to 100% mobile-phase B. Next, 100% mobile-phase B was maintained for 20 min. The respective flow rate gradient during these two phases, changes from 1 ml min^{-1} to 2 ml min^{-1}. At the end of the 50-minute run, the column was rinsed for 15 min by linear ramping back to 85% mobile-phase A within 5 min and maintaining this for 10 min (Lami et al., 2000).

Chromatogram evaluation and error calculation

Baseline chromatograms of two samples from the composite core (located at 14.36 ka BP and 15.85 ka BP) are displayed below. The Full Chemical Error (FCE) was calculated as the mean absolute error (MAE) of 5 random full chemical duplicate samples (separate samples at the same depth; $original = S_i;\ duplicate = D_i$). When the FCE expressed as a percentage of the downcore range (max value in timeseries S – min value) was >35% the pigment timeseries were excluded. $FCE = \frac{\sum_{i=1}^{5} \sqrt{(S_i - D_i)^2} / 5}{\max(S) - \min(S)} \cdot 100\%$

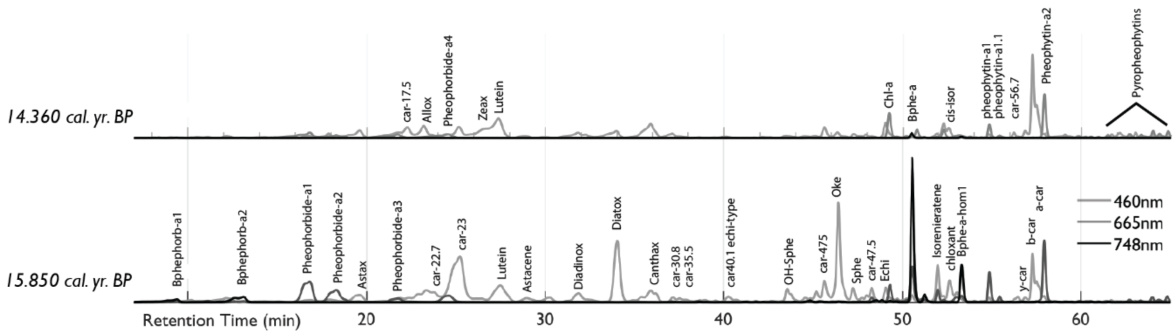

Table S1: ^{14}C dates, tephra and biostratigraphic markers used for the age-depth model presented in Fig. 2 of the main text. One sample (BE-20927) was lost during target pressing. The sample BE-20934.1.1 (*Pinus sp.* periderm) was excluded because it is too young (10.9 ka BP) relative to its stratigraphic position (ca. 16.7 ka BP).

Lab Code	Master depth (cm)	^{14}C Age uncal. (y BP)	±1s (y)	Calibrated Age Intcal20 (cal. BP)	±1sigma	Mean modelled age	±	Measurement	Macrofossil	Weight (dry)	Comment
BE-20926.1.1	487.7	9362	105	10580	10409-10733	10642	307	gas	5 c.f. wood fragments, thin, rather soft (8 mm²),	0.2 mg	
BE-20927	495.6	-	-	-	-	10992	342.5	graphite	3 *Pinus sp.* periderm fragments (15 mm²); conif. scale, *Quercus sp.* Budscale; deciduous twig; small dicot leaf fragments; *Betula alba* fruit, *Betula alba* (woody fruit scale)	0.8 mg	lost during target pressing
BE-20928.1.1	504.8	10005	56	11839	11330-11685	11599	227.5	graphite	*Pinus sp.* Periderm; wood fragment (14 mm²)	1.1 mg	
BE-20929.1.1	508.7	10155	56	11494	11330-11654	11830	262.5	graphite	several *Pinus sp.* periderm fragments (90 mm²); *Betula alba* fruit; 2 conif. (*P.cembra*) basis of male blossom; 4 conif. scale fragments	1.6 mg	
BE-21037.1.1	514	10214	115	11912	11624-12431	12261	448.5	gas	*Pinus sp.* periderm thin fragments (10 mm²)	0.4 mg	
LST	520.2			13006	12997-13015	13062	55	TEPHRA	Reinig et al., 2021	-	
BE-21036.1.1	525.4	11398	130	13282	13165-13408	13405	183.5	gas	*Pinus sylvestris* type short shoot with two needle fragments (basis)	0.3 mg	
PIN_67.6	527.7			13753	13584-13922	13689	309	BIOSTRAT	Amman et al., 2013	-	
BE-20930.1.1	527.7	11508	134	13378	13242-13496	13689	309	gas	11 *Betula alba* fruits (partly with wings)	0.4 mg	
BE-20931.1.1	532.7	12280	123	14331	14057-14800	14212	270.5	gas	4 *Betula alba* fruit fragments; few small dicot leaf fragments	0.1mg	
BET_75.5	535.2			14443	14254-14632	14461	291.5	BIOSTRAT	Amman et al., 2013	-	
BE-20932.1.1	537.7	12282	283	14418	13877-14907	14675	312.5	gas	1 *Betula alba* fruit fragment (without wings)	0.1mg	
JUN_78.5	538.2			14665	14476-14854	14711	339.5	BIOSTRAT	Amman et al., 2013	-	
BE-20933.1.1	542.7	12573	145	14849	14481-15183	14989	405.5	gas	Conif. deciduous twig with periderm; conif. deciduous small fragments (3 mm²)	0.6 mg	
BET_88.5	548.2			16000	15315-16685	15575	804	BIOSTRAT	Rey et al., 2020	-	
BE-20934.1.1	560.7	9555	302	10886	10413-11251	16680	1305.5	gas	Conif. *Pinus sp.* Periderm (0.5 mm²)	<0.1mg	outlier

Table S2: Parameters used for RABD index calculations.

Name	Pigment	Left band (nm)	Max. absorption (nm)	Right band (nm)
Rmean	Reflectance	471		950
$RABD_{844}$	Bphe *a*	772	844	900
$RABD_{619}$	Phycocyanin	570	619	634
$RABD_{667}$	Chlorophyll *a*	634	667	772

Table S3: Table with pigments and their primary producers and interpretation, retention times and calibration parameters. Ward's clustering on carotenoids yielded 4 carotenoid groups (Fig. 6 main text) which were subdivided into subgroups based on the primary producer interpretations.

Carotenoid groups	Pigment name	Retention time (Lami et al., 2000)	Calibration (y = ax +b)	Primary producers*
1	Okenone	46.3	a = 0.1500 b = 0.000	PSB
1	Spheroidene	47.2	β-car	PNSB[2], N-fixing
1	unknown	45.0, 45.6	β-car	
2.1	Isorenieratene	51.9	a = 0.1740 b = 0.0350	GSB, steptomycetaceae, mycobacteria[1]
2.1	OH-spheroidene	43.5	β-car	PNSB[2], N-fixing
2.1	unknown	40.2, 48.2, 49.6, 56.4	β-car	
2.2	Diatoxanthin	34	β-car	Diatoms, Silicifyers
2.2	unknown	23.7, 24.6, 25.1	β-car	
3.1	Chloroxanthin	52.6	β-car	PNSB[2], N-fixing
3.1	α-carotene	57.5	β-car	
3.1	unknown	47.9	β-car	
3.2	Diadinoxanthin	31.8	a = 0.1363 b = 0.0171	Dinoflagellates, diatoms, green algea
3.2	β-carotene	57.3	a = 0.1294 b = 0.0177	All aquatic primary producers
3.2	Lutein, Zeaxanthin	27.4, 26.6	a = 0.1220 b = 0.0950	Euglinids, green algea, eustigmacaea
3.2	unknown	16.8, 22.3, 35.6, 35.9, 37.1	β-car	
4.1	Astaxanthin	19.6	β-car	Stresssed green algea[3]
4.1	Astacene	28.9	β-car	
4.1	unknown	19.2	β-car	
4.2	Canthaxanthin	36.1	a = 0.1187 b = 0.0249	Filamentous cyanobacteria, N-fixing
4.2	Alloxanthin	23.2	a = 0.0904 b = 0.1147	Cryptophytes, Silicifyers
4.2	γ-carotene	56.9	β-car	
4.2	unknown	21.2, 21.8, 37.6, 43.0, 56.2, 61.9, 63.0, 34.4	β-car	
4.3	Echinenone	49	a = 0.3000 b = 0.0480	Cyanobacteria
4.3	unknown	51.4, 53, 59.8	β-car	
	Chlorophyll *a*	49.2, 50.2, 50.8	a = 0.2582 b = -0.0008	Green primary producers
	Pheophorbides *a*	All greens between 10.8 - 49.6	chl *a*	Chl *a* degradation by grazing[4] (Zooplankton)
	Pheophytins *a*	All greens between 51.8 - 59.9	chl *a*	Chl *a* degradation by light and oxygenation
	Pyropheophytin *a*	All greens between 60.5 - 64.8	chl *a*	Heavy chl *a* degradation (e.g. terrestrial inwash)
	Bacteriopheophytin *a*	50.5, 51.1, 53.3	β-car	PSB
	Bacteriopheophorbide *a*	9.4, 13.1	β-car	PSB

* Based on classification schemes of Yabuzaki (2017); Bianchi and Canuel (2011); Schlüter et al. (2006); Lami et al. (2000).

[1] Mycobacteria abundance in many freshwater ecosystems and pigment production is proven (Becerril et al., 2018; Vaerewijck et al., 2005; Joynson, 1979; David, 1974).

[2] Albrecht et al., (1997); Davies et al. (1969).

[3] Orosa et al. (2001); Boussiba and Vonshak (1991); Renstrøm et al. (1981)

[4] Bianchi and Canuel (2011)

Figure S1: Core segments, stratigraphic correlation and composite core of Amsoldingersee (coring August 2022)

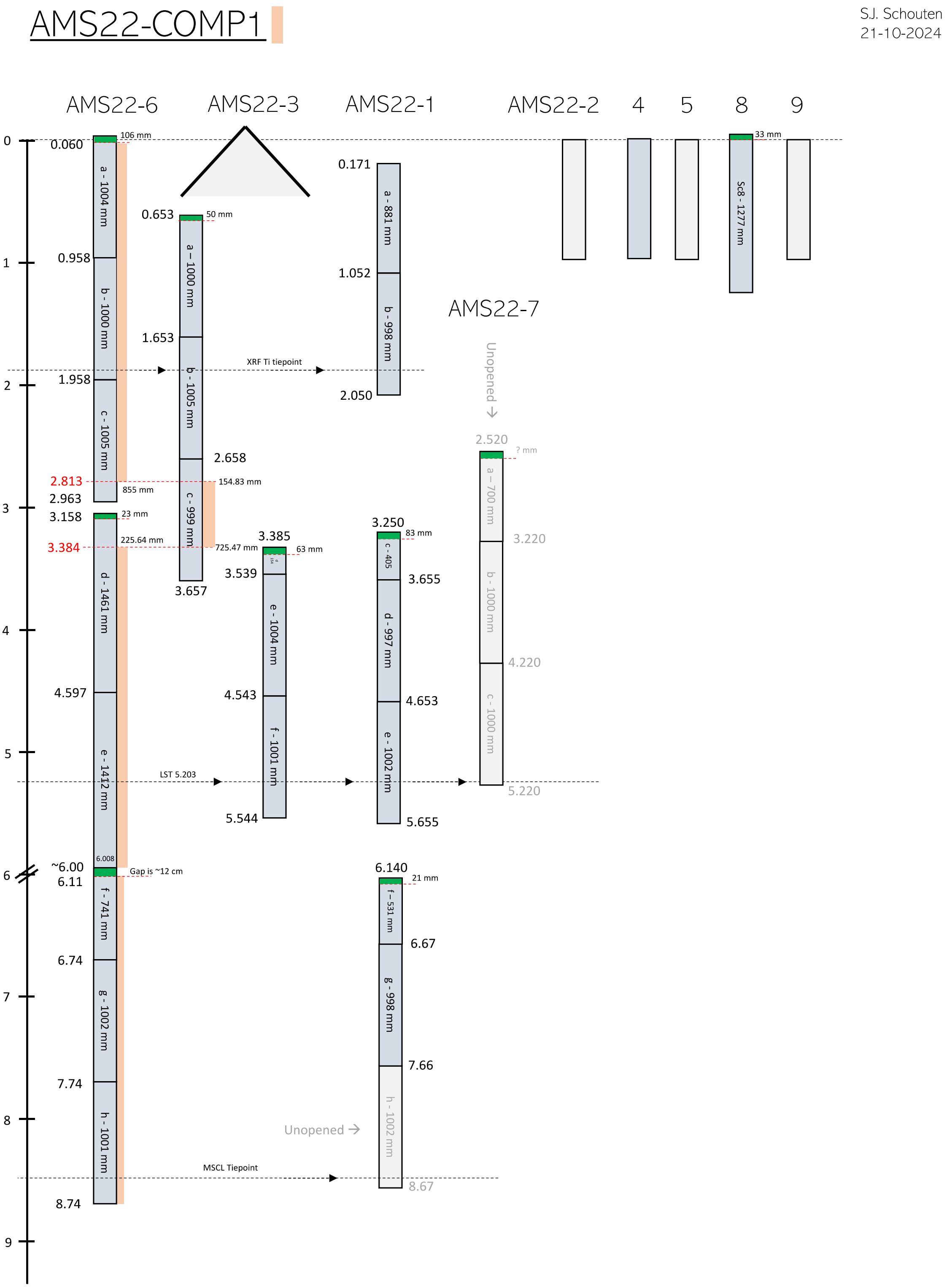

Figure S2: Calibration of RABD844 (inferred from hyperspectral imaging) to Bphe *a* measured with UV-VIS (spectrophotometry) after pigment extraction (proxy-proxy calibration, Butz et al., 2015). Fig. S2 (left) shows the regression with 95% confidence (dashed line) and prediction intervals (dotted line) and the calibration statistics (n, p-values, R^2_{adj}, RMSEP for 10-fold jackknifing, k-fold jackknifing, and bootstrapped); the orange horizontal dashed line represents the Limit of Quantification. The panels in the middle show the Q-Q plot, Cook's Distance, the time series comparison, the residual distribution and (right panels) the scale-location, residual trajectory and leverage plots.

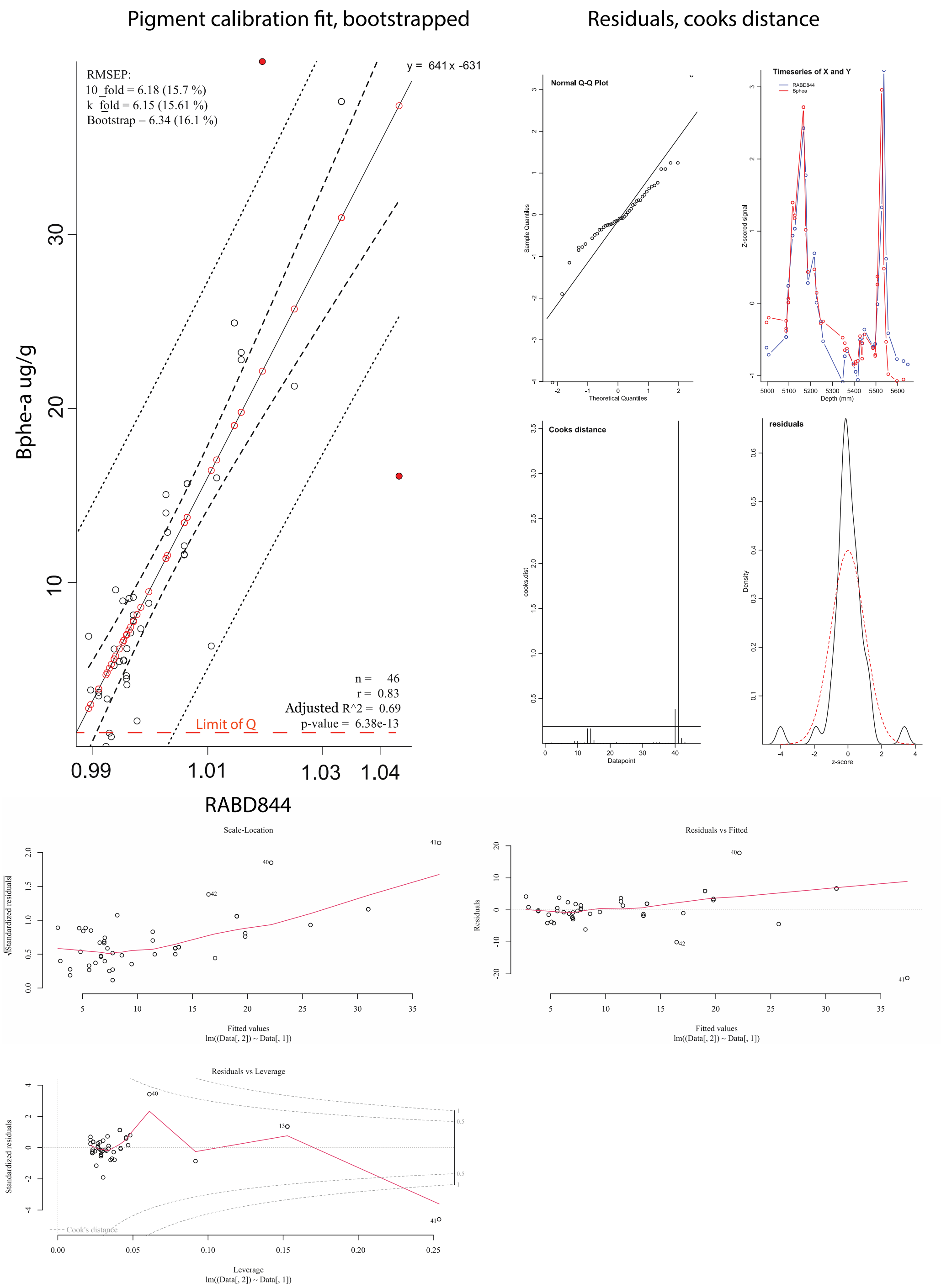

Figure S3: Calibration of RABD667 (inferred from hyperspectral imaging) to chl *a* measured with UV-VIS (spectrophotometry) after pigment extraction (proxy-proxy calibration, Butz et al., 2015). Fig. S3 (left) shows the regression with 95% confidence (dashed line) and prediction intervals (dotted line) and the calibration statistics (n, p-values, R^2_{adj}, RMSEP for 10-fold jackknifing, k-fold jackknifing, and bootstrapped); the orange horizontal dashed line represents the Limit of Quantification. The panels in the middle show the Q-Q plot, Cook's Distance, the time series comparison, the residual distribution and (right panels) the scale-location, residual trajectory and leverage plots.

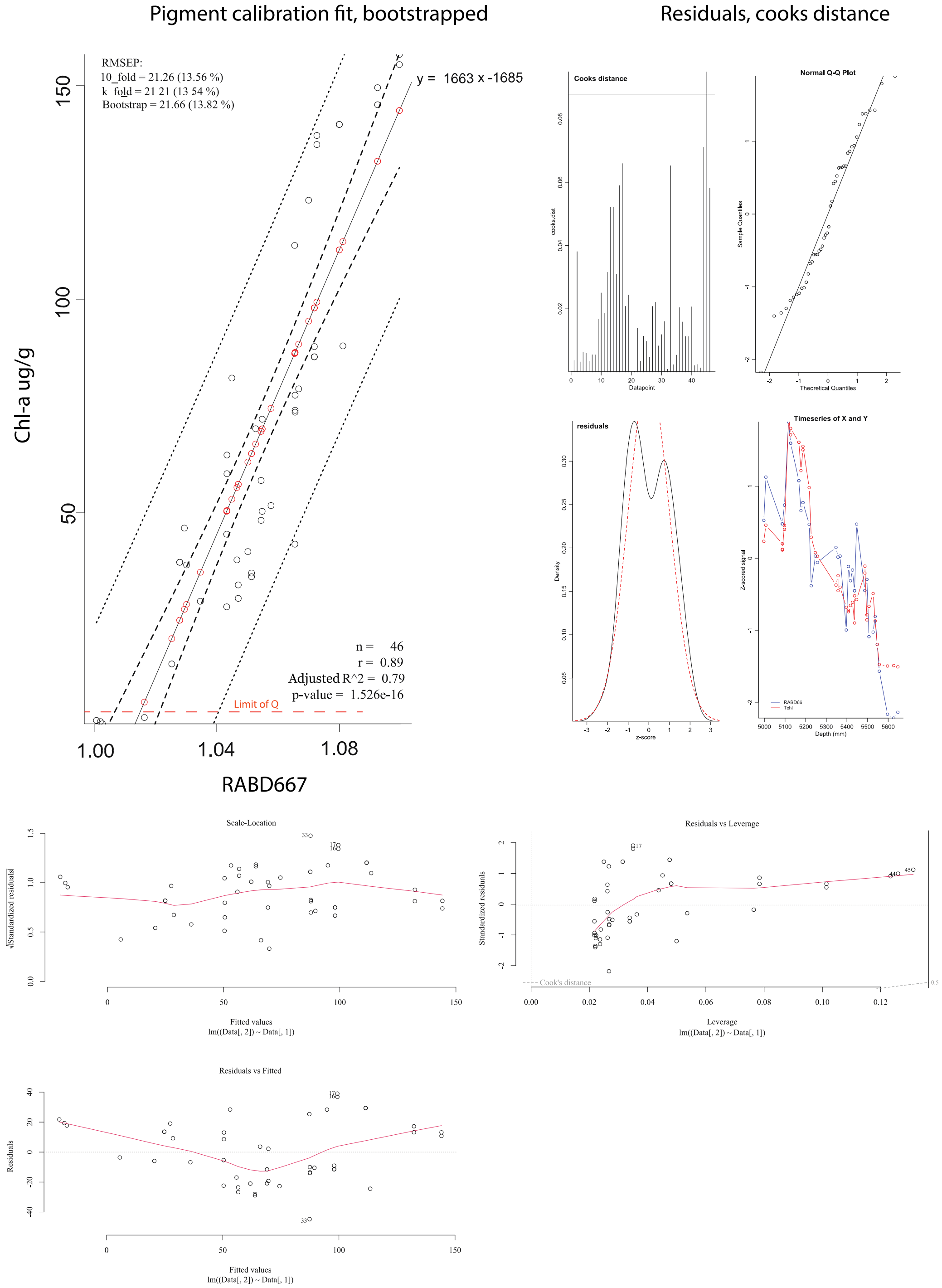

Figure S4: Pollen diagram of AMS22-COMP1 and biostratigraphic markers. Pollen analysis followed Moore et al. (1991). From the pollen diagram we inferred four established biostratigraphic markers (horizontal dashed lines) after Rey et al. (2017, 2020), Ammann et al. (2013) and Wehrli et al. 2007) – Early *Betula* appearance, *Juniperus* rise, main *Betula* rise, *Betula - Pinus* shift:

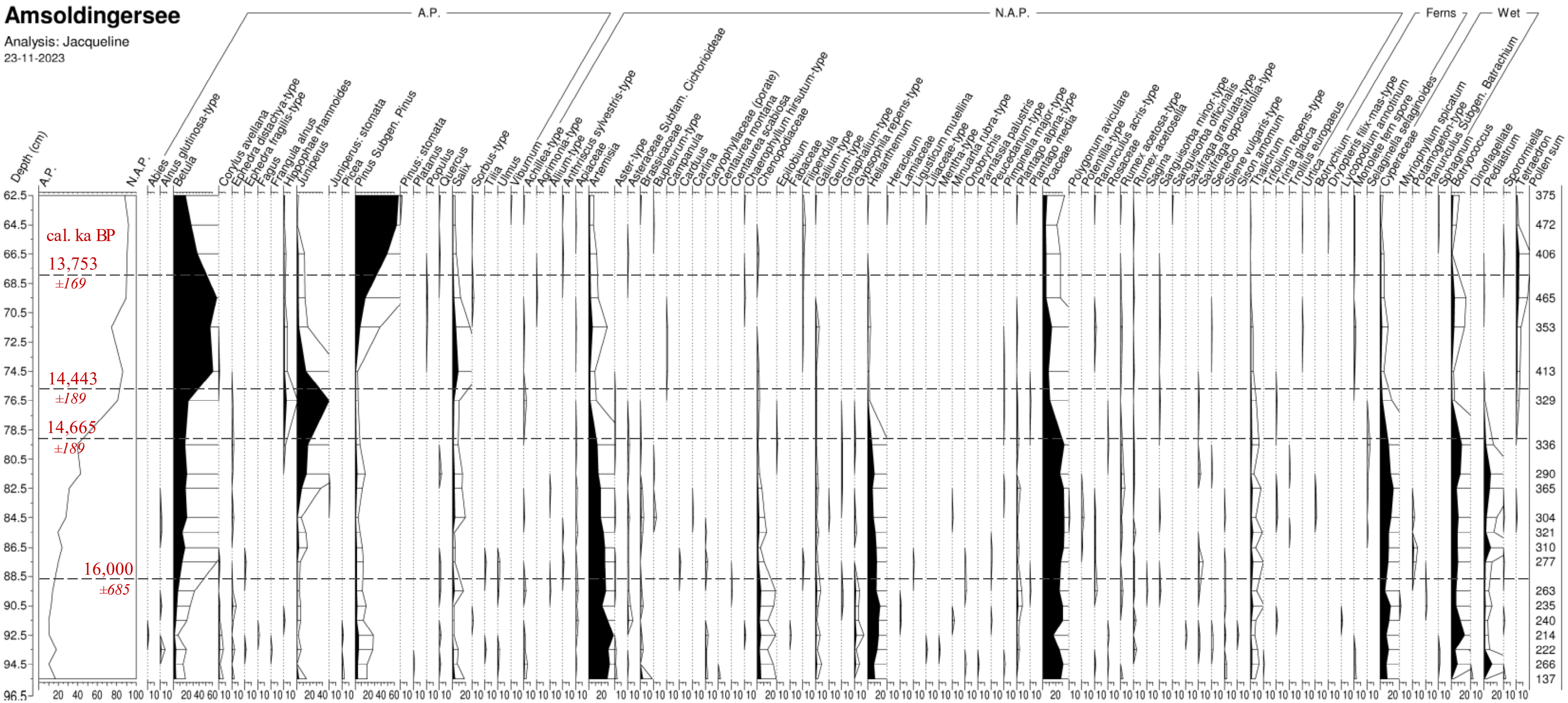

Figure S5: All CLR XRF data from core AMS22_COMP1. A selection is shown in Fig. 3 of the main text.

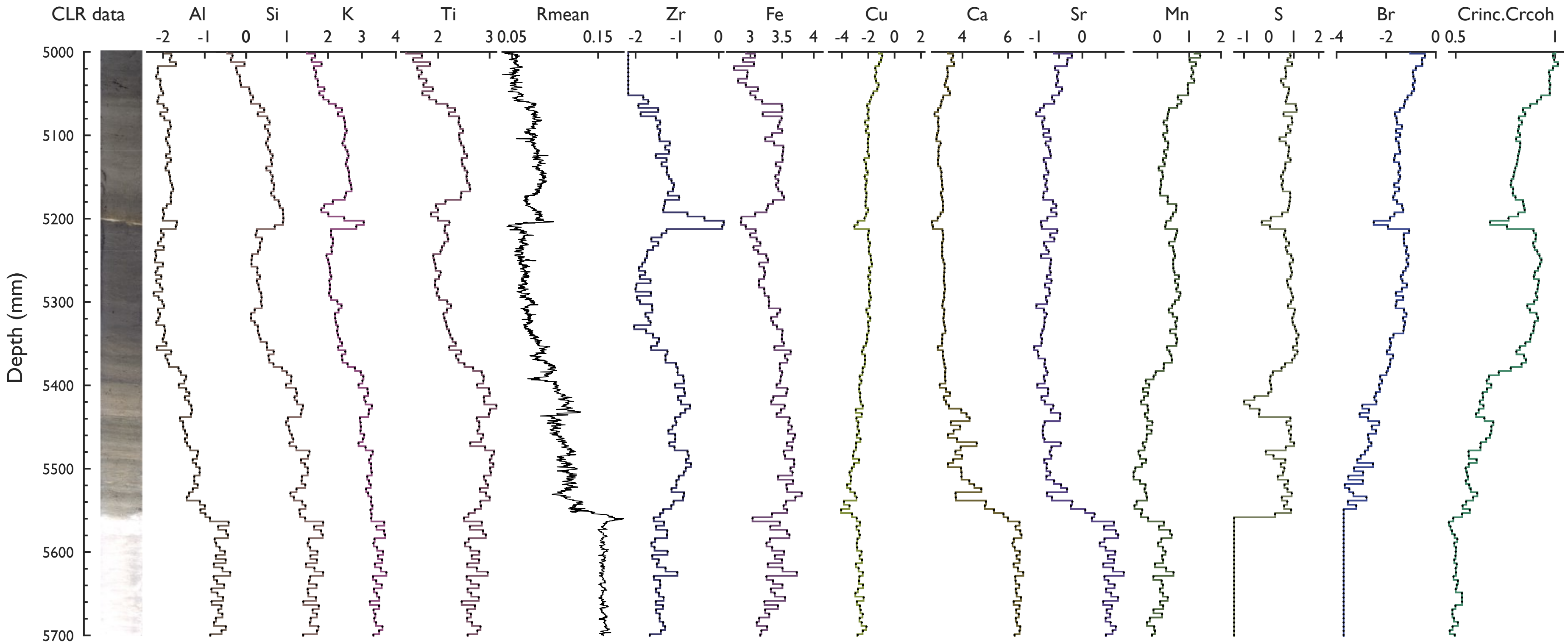

Figure S6: 'Standardized' Euclidian multi-dimensional scaling was applied to the dataset to check for non-linear dependencies. Added are the resulting MDS axes and the inferred clusters (lithotypes) that remain well separated when applying MDS. The stress plot is provided with an appropriate cutoff at 0.05 indicating that only two MDS components are needed to explain most data variance.

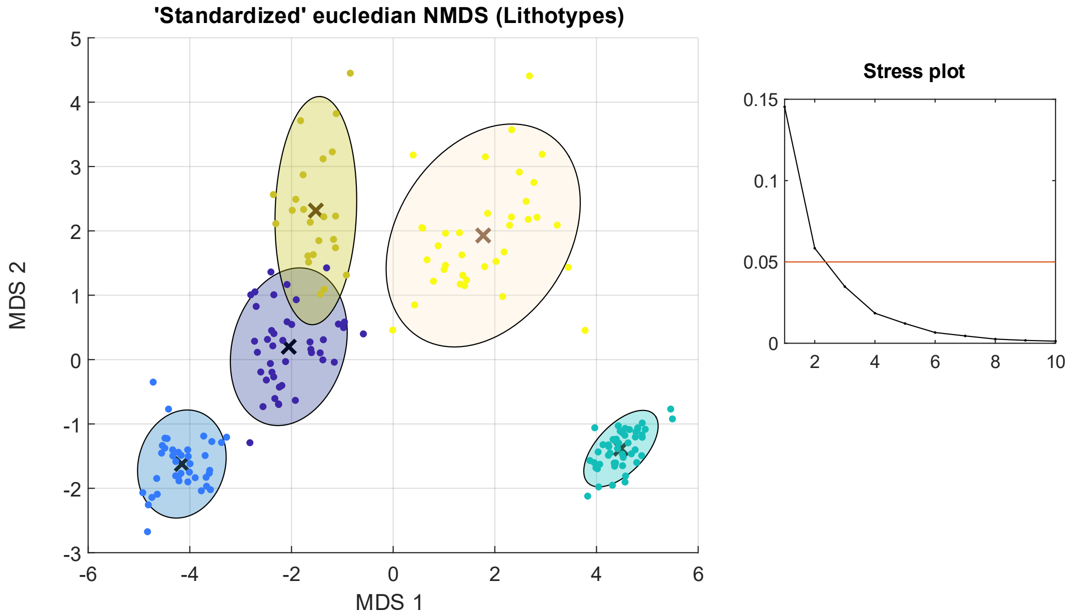

Figure S7: PC biplot of P, Mn and Fe fractions (all data). Ward's clusters 1–4 are colored along their confidence ellipses. Arrows indicate the temporal trajectory (ages in green). The environmental interpretation of the PCs is indicated in blue text.

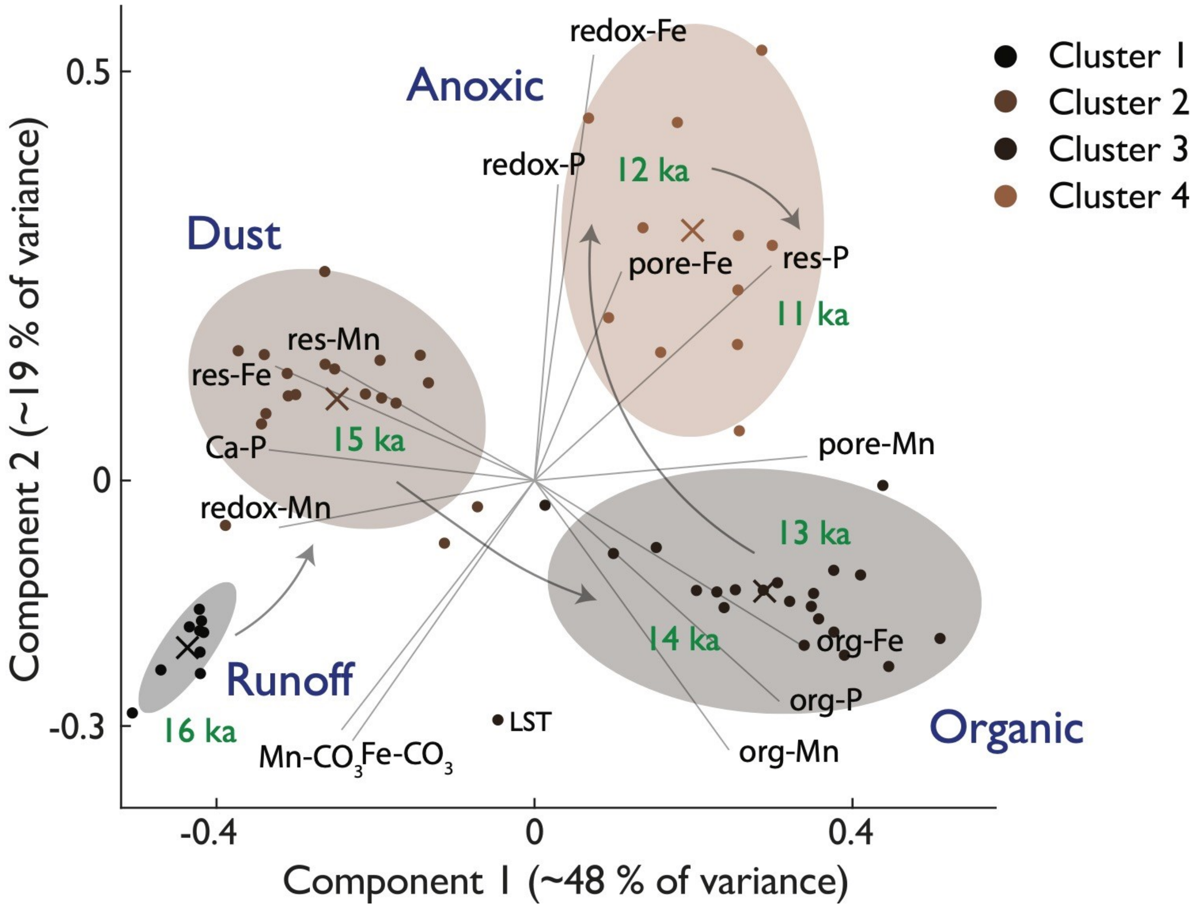

Figure S8: Pigment stratigraphy for a) carotenoids and b) photopigments of lake Amsoldingen (AMS22-COMP1)

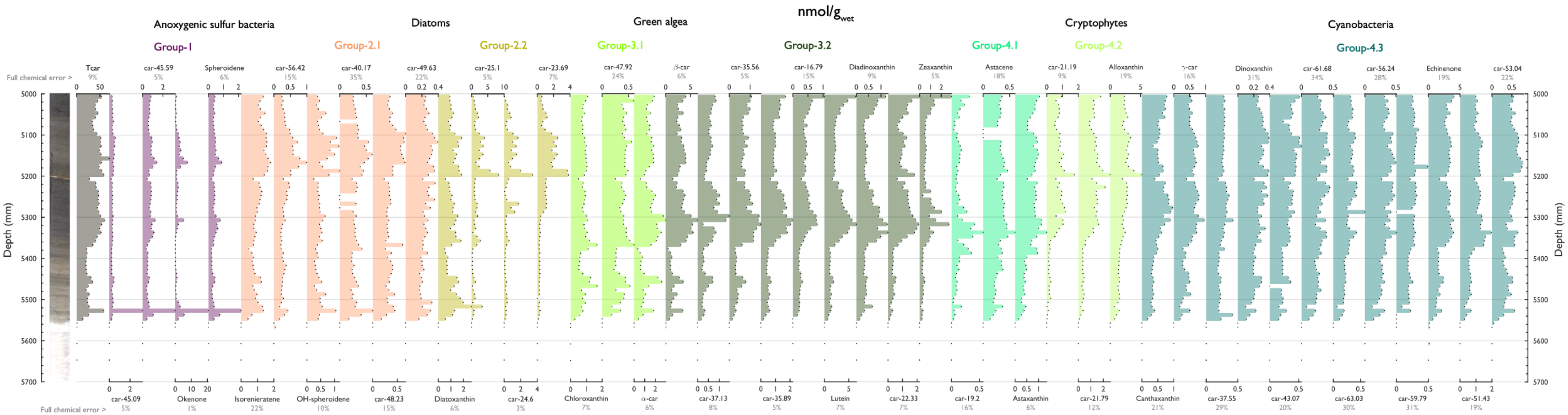

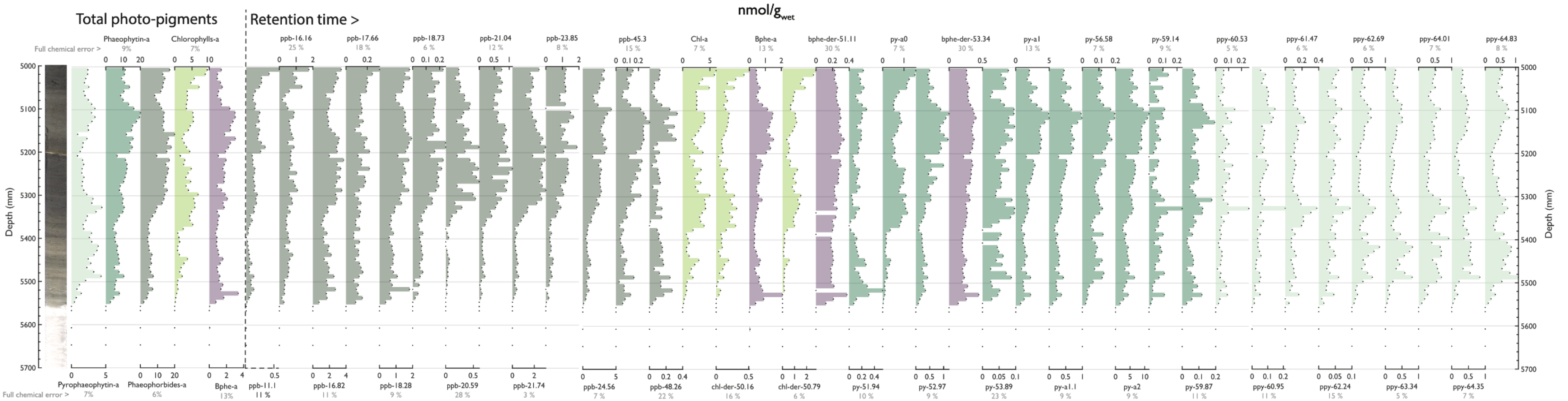

Figure S9. Redundancy analysis was performed on the Hellinger transform of the carotenoid dataset and total sums of pheophorbides, pheophytins, pyropheophytins and chlorophylls *a*. The RDA was first run (**A**) using the following explanatory variables: JulyT (merged by overlaying data from Bolland et al., 2020 and the Alpine stack from Heiri et al., 2015; pre 14.8 ka BP from Bürgaschisee, post 14.8 ka BP from Alpine stack. We further smoothened the data using the 'rloess' method with a span of 2% for the alpine stack and 20% for the Bürgaschisee data; Arboreal Pollen AP from Moossee (Rey et al., 2020); $\delta^{18}O$ of NGRIP (NGRIP Members, 2004), Bphe *a* (this study) and TN, TS, TOC and CNS (this study). The variance partitioning between nutrients and temperature is shown panel **B**. A second RDA (panel **C**) and was performed after forward selection (Legendre, 2012).

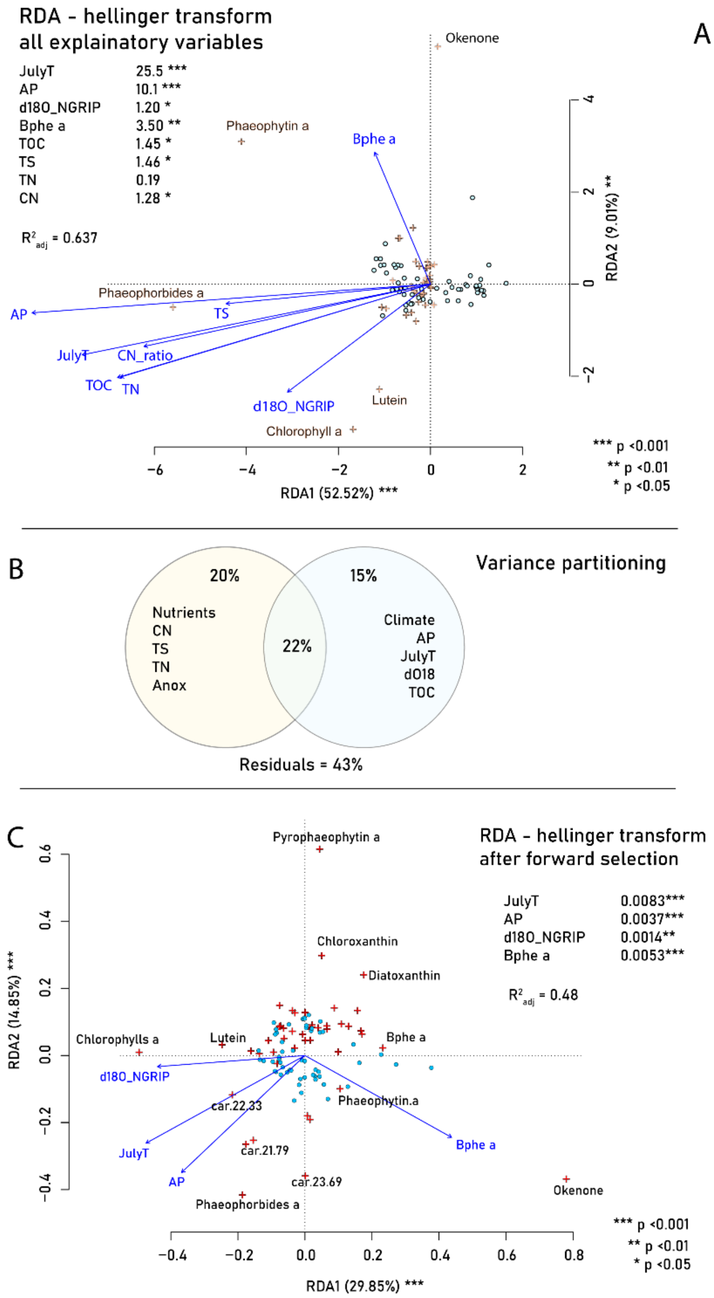

Figure S10. PC1 versus PC2 loadings for all extracted pigments. Only the identified pigments are named.

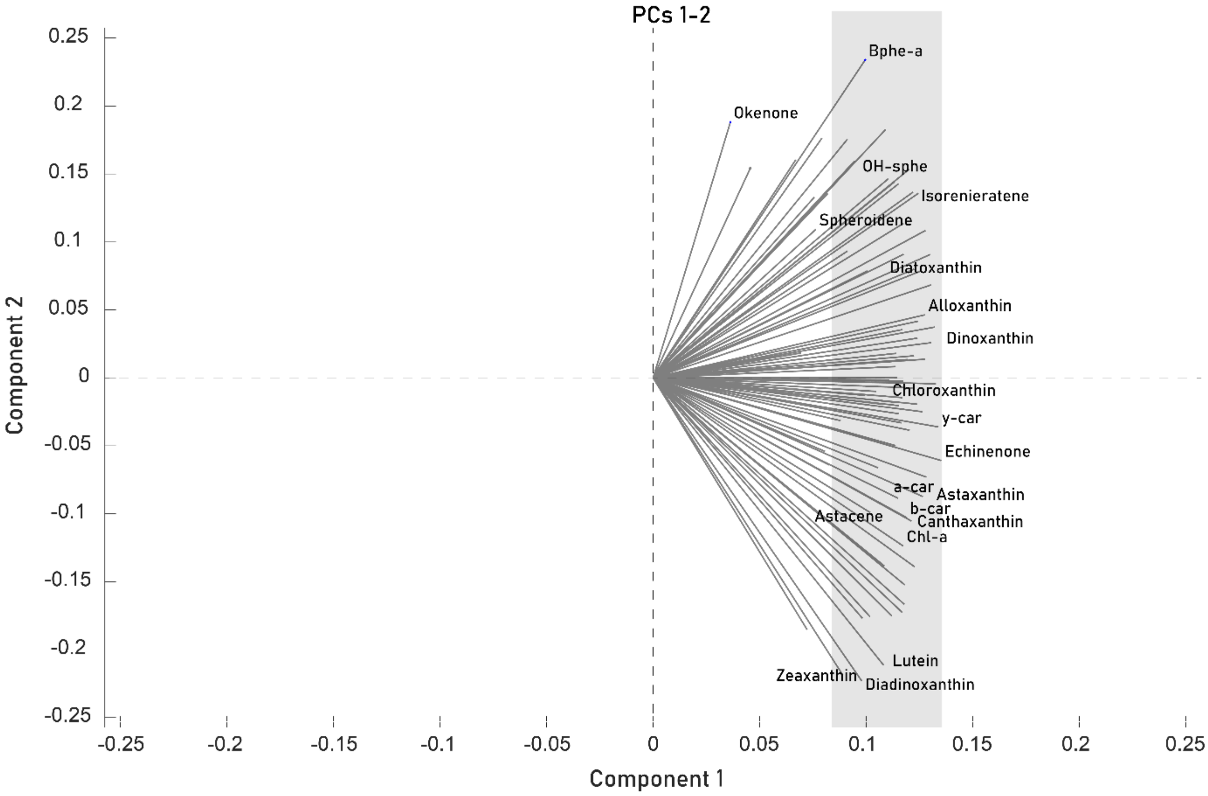

References (SOM)

Albrecht, M., Ruther, A., Sandmann, G. (1997). Purification and biochemical characterisation of a hydroxyneurosporene desaturase involved in the biosynthetic pathway of the carotenoid spheroidene in *Rhodobacter sphaeroides*. Journal of Bacteriology, 179(23), 7462-7467, 10.1128/jb.179.23.7462-7467.1997, 1997.

Ammann, B., van Leeuwen, J. F., van der Knaap, W. O., Lischke, H., Heiri, O., Tinner, W.: Vegetation responses to rapid warming and to minor climatic fluctuations during the Late-Glacial Interstadial (GI-1) at Gerzensee (Switzerland). Palaeogeography, Palaeoclimatology, Palaeoecology, 391, 40–59, 10.1016/j.palaeo.2012.07.010, 2013.

Becerril, A., Álvarez, S., Braña, A. F., Rico, S., Díaz, M., Santamaría, R. I., Salas, J. A., Méndez, C.: Uncovering production of specialised metabolites by *Streptomyces argillaceus*: Activation of cryptic biosynthesis gene clusters using nutritional and genetic approaches. *PLoS One*, 13(5), e0198145, 10.1371/journal.pone.0198145, 2018.

Bianchi, T. S., and Canuel, E. A.: Photosynthetic Pigments: Chlorophylls, Carotenoids, and Phycobilins in: Chemical Biomarkers in Aquatic Ecosystems, edited by: Bianchi, T. S., Canuel, E.A., 221-247, Princeton University Press, https://doi.org/10.1515/9781400839100, 2011

Bolland, A., Rey, F., Gobet, E., Tinner, W., and Heiri, O.: Summer temperature development 18,000–14,000 cal. BP recorded by a new chironomid record from Burgäschisee, Swiss Plateau. Quaternary Science Reviews, 243, 106484, 10.1016/j.quascirev.2020.106484, 2020.

Boussiba, S., Vonshak, A.: Astaxanthin accumulation in the green alga *Haematococcus pluvialis*. Plant and cell Physiology, 32, 1077–1082, 10.1093/oxfordjournals.pcp.a078171, 1991.

Butz, C., Grosjean, M., Fischer, D., Wunderle, S., Tylmann, W., Rein, B.: Hyperspectral imaging spectroscopy: a promising method for the biogeochemical analysis of lake sediments. Journal of Applied Remote Sensing, 9, 096031, 10.1117/1.JRS.9.096031, 2015.

David, H. L.: Carotenoid pigments of *Mycobacterium kansasii*. Applied Microbiology, 28(4), 696-699, https://doi.org/10.1128/am.28.4.696-699.1974, 1974.

Davies, B. H., Holmes, E. A., Loeber, D. E., Toube, T. P., Weedon, B. C. L.: Carotenoids and related compounds. Part XXIII. Occurrence of 7, 8, 11, 12-tetrahydrolycopene, spheroidene, 3, 4, 11′, 12′-tetrahydrospheroidene, and 11′, 12′-dihydrospheroidene in *Rhodospirillum rubrum*. Journal of the Chemical Society C: Organic, (9), 1266-1268, https://doi.org/10.1039/J39690001266, 1969.

Heiri, O., Ilyashuk, B., Millet, L., Samartin, S., Lotter, A. F.: Stacking of discontinuous regional palaeoclimate records: Chironomid-based summer temperatures from the Alpine region. The Holocene*, 25*, 137–149, 10.1177/0959683614556382, 2015.

Joynson, D. H. M.: Water: The natural habitat of *Mycobacterium Kansasii*? Tubercle, 60(2), 77-81, https://doi.org/10.1016/0041-3879(79)90039-4, 1979.

Lami, A., Guilizzoni, P., Marchetto, A.: High resolution analysis of fossil pigments, carbon, nitrogen and sulphur in the sediment of eight European Alpine lakes: The MOLAR project. Journal of Limnology*, 59*, 15–28, 10.4081/jlimnol.2000.s1.15, 2000.

Legendre, P.: Numerical ecology*.* Elsevier, 10.1016/b978-0-12-409548-9.10595-0, 2012.

Moore, P. D., Webb, J. A., Collison, M. E.: Pollen analysis*.* (Vol. 80). *JSTOR,* 10.2307/2260877, 1991.

North Greenland Ice Core Project members.: High-resolution record of Northern Hemisphere climate extending into the last interglacial period. Nature, *431*, 147–151, 10.1038/nature02805, 2004.

Orosa, M., Valero, J. F., Herrero, C., Abalde, J.: Comparison of the accumulation of astaxanthin in *Haematococcus pluvialis* and other green microalgae under N-starvation and high light conditions. Biotechnology Letters, *23*, 1079–1085, https://doi.org/10.1023/A:1010510508384, 2001.

Renstrøm, B., Borch, G., Skulberg, O. M., Liaaen-Jensen, S.: Optical purity of (3S, 3'S)-astaxanthin from *Haematococcus pluvialis*. Phytochemistry, 20(11), 2561-2564, https://doi.org/10.1016/0031-9422(81)83094-4, 1981.

Rey, F., Gobet, E., Schwörer, C., Hafner, A., Szidat, S., Tinner, W.: Climate impacts on vegetation and fire dynamics since the last deglaciation at Moossee (Switzerland). Climate of the Past, 16, 1347–1367, 10.5194/cp-16-1347-2020, 2020.

Rey, F., Gobet, E., van Leeuwen, J. F., Gilli, A., van Raden, U. J., Hafner, A., Othmar, W., Rhiner, J., Schmocker, D., Zünd, J., Tinner, W.: Vegetational and agricultural dynamics at Burgäschisee (Swiss Plateau) recorded for 18,700 years by multi-proxy evidence from partly varved sediments. Vegetation History and Archaeobotany, 26, 571–586, 10.1007/s00334-017-0635-x, 2017.

Schlüter, L., Lauridsen, T. L., Krogh, G., Jørgensen, T.: Identification and quantification of phytoplankton groups in lakes using new pigment ratios–a comparison between pigment analysis by HPLC and microscopy. Freshwater Biology, 51, 1474–1485, 10.1111/j.1365-2427.2006.01582.x, 2006.

Vaerewijck, M. J., Huys, G., Palomino, J. C., Swings, J., Portaels, F.: Mycobacteria in drinking water distribution systems: ecology and significance for human health. FEMS Microbiology Reviews, 29(5), 911-934,10.1016/j.femsre.2005.02.001, 2005

Wehrli, M., Tinner, W., Ammann, B.: 16.000 years of vegetation and settlement history from Egelsee (Menzingen, central Switzerland). The Holocene, *17*, 747–761, 10.1177/0959683607080515, 2007.

Yabuzaki, J.: Carotenoids Database: structures, chemical fingerprints and distribution among organisms. Database, bax004 [data base], 10.1093/database/bax004, 2017.